Chapter 1

Introduction

1.1 Introduction of Tungstate – A General Background

It is known that tungstate is a very important family of inorganic materials that has wide applications in many fields, such as Photoluminescence, Microwave applications, Optical fibres, Scintillator materials, Humidity sensors, Catalysis, etc. As a self-activating phosphor, tungstate has some advantages, e.g. high chemical stability, high X-ray absorption coefficient, high Light Yield, and low afterglow to luminescence. Tungstate crystals can be divided in two groups: Scheelite ($CaWO_4$, $BaWO_4$ and $PbWO_4$) and Wolframite ($MgWO_4$, $ZnWO_4$ and $CdWO_4$). $BaWO_4$ shows very weak luminescence at liquid helium temperature which vanishes at room temperature. $MgWO_4$ is used at photoluminophor already for a long time [1]. $ZnWO_4$ and $CdWO_4$ are perspective materials in the field of computer tomography [2]. $CaWO_4$ is an effective luminophor which is used for more than hundred years in medical purpose and in luminescence lamp but it has slow luminescence decay (about 100μs) restrict its use in optical devices based on low time resolution.

Hence out of all tungstates, $PbWO_4$ become a subject of renewed interest about 15 years ago when its favorable characteristics as scintillation detector was reported. Though $PbWO_4$ has low light yield (100 time smaller than $CaWO_4$), it has very short decay time (ns) makes it strongest candidate for scintillation detector. High density of $PbWO_4$ also favors its use in high energy physics and medical application. There are hundreds of papers already published on $PbWO_4$ large single crystals but very few papers are reported on $PbWO_4$ with nanometer range, particularly on Cerium doped $PbWO_4$ nanophosphor. Large single crystals of $PbWO_4$ are produced either via Czochralski or Bridgman method which require highly expensive and specially designed equipments. These methods produce PbO and WO_3 harmful gases during crystal growth due to higher synthesis temperature (i.e.1125°C). Moreover, $PbWO_4$

crystals obtained from these methods presents several problems, such as: inhomogeneity, impurity contamination and powders with different sizes and non-uniform distribution. Products obtained by these methods are in bulk size which cannot be used for devices based on nano dimensions. These limitations lower the applicability of these methods for large scale production of $PbWO_4$ crystals.

Since $PbWO_4$ Phosphor has structure sensitivity and its luminescence properties remarkably affected by structure defects present in the crystal. We can improve its scintillating properties through changing and controlling its structure defects, such as appropriate doping and controlling synthesis temperature. Doping with rare earth ions adjust the defects in the Pure $PbWO_4$ and eliminate some harmful defects. Earlier studies found that some related experimental parameters including the concentration of the anionic surfactant, the water content, and reaction temperature have great influences on the product morphology. By carefully controlling these experimental parameters, $PbWO_4$ nanostructures with morphologies of bundles of rods, ellipsoids, spheres, bipyramids, and nanoparticles can be efficiently achieved. Cerium has been tried as a beneficial rare earth doping impurity recently. Cerium oxide (CeO2), one of the most important rare-earth oxides, has earned intensive interest in the past decades for its vital roles played in some emerging fields including environmental and energy related applications. Recent development in nanotechnology requires $PbWO_4$ material having different morphologies and dimensions suitable for nano-devices. So it is important to study effect of different reaction parameters (Precursor, pH, Concentration, Time and Temperature) on morphology of the final product. Interesting applications of bulk sized $PbWO_4$ and less reported properties of undoped and Cerium doped $PbWO_4$ with nano dimensions motivate us to perform research work presented in this thesis.

To study the effect of different reactants, temperature and pH of reaction media on the structural and Optical properties of $PbWO_4$ and Cerium doped $PbWO_4$ phosphor.

OBJECTIVES AND SCOPE OF THE WORK

In order to achieve this aim, following objectives have been set.

- To design and develop Teflon Lined Stainless Steel Autoclave which is efficiently able to synthesis $PbWO_4$ phosphor.
- To synthesis undoped and Cerium doped $PbWO_4$ phosphor with different Lead Sources, at reaction Temperature and pH of solution with Autoclave by Low temperature Hydrothermal Method.
- Characterization of as prepared samples with X-ray Diffraction (XRD), Transmission Electron Microscopy (TEM), Scanning Electron Microscopy (SEM) for structural studies.
- Characterization of as prepared samples with Photoluminescence (PL) for optical studies.

1.2 Lead Tungstate – $PbWO_4$

Lead Tungstate $PbWO_4$ (PWO) occurs in the nature as tetragonal stolzite with scheelite type structure (space group $I4_{1/}a$) and monoclinic raspite with wolframite type structure (space group $P2_{1/}a$). Raspite phase transforms irreversibly to the stolzite one at about 400°C [3]. The first information on the emission properties of PWO is dated as early as the late 1940s [4]. Compared to other well-known scintillators such as BaF_2, CeF_3 and CsI, $PbWO_4$ phosphor is most attractive for its high-energy physics application because of its high density (8.3 g cm^{-3}), short decay time (less than 10 ns for a large light output), high irradiation damage resistance (10^7 rad for undoped and 10^8 rad for La doped $PbWO_4$), small moliere radius, fast decay time, non-hygroscopicity and low production cost [5-7]. $PbWO_4$ shows interesting excitonic luminescence, Thermoluminesce and stimulated Raman Scattering behavior [8, 9]. Lead tungstate crystals are fast and dense scintillators found an application for high energy electromagnetic calorimeter of Compact Muon Solenoid (CMS) detector at Large Hedron Collider (LHC) at Center of Europe for Research Nuclear (CERN).

1.3 History of Synthesis

Generally $PbWO_4$ are grown from expensive methods, such as: high temperature solid-state reaction [10-12], flux method for whisker growth [13], from the melt using the Czochralski method [14–17], Bridgman method [18] and from the high temperature strain (HTS) [19]. Tungstate thin films have been prepared by reacting various metal oxide thin film with WO_3 vapor [20]. Most of these methods require high temperature heating. At high temperature there is a tendency for the WO_3 group to evaporate, resulting inhomogeneous composition of tungstates.

These methods require highly expensive and specially designed equipments for crystal growth. Evaporation of harmful gases such as PbO and WO_3 during crystal growth due to higher synthesis temperature also lowers applicability of these methods for large scale production of $PbWO_4$ crystals. $PbWO_4$ crystals obtained from these methods presents several problems, such as: inhomogeneity, impurity contamination and powders with different sizes and nonuniform distribution. Moreover, products obtained by these methods are in bulk sized which cannot be used for devices which are based on nano dimensions.

To minimize these problems, soft chemical methods such as: sol–gel [21], sonochemical route [22, 23], microemulsion [23], microwave assisted route [24,25,26] and hydrothermal [27-30] have been employed to control with accuracy the chemical composition, homogeneity, microstructure, physical and chemical characteristics.

SOME METHODS USED FOR NANOMATERIAL SYNTHESIS

Plasma arcing

In Plasma arcing molecules and atoms are separated by vaporization and then allowed to deposit in a carefully controlled and orderly manner to form nanoparticles. Plasma is achieved by making inert gas conduct electricity by providing a potential difference across two electrodes. In arc discharge method, two high purity graphite electrodes as anode and cathode are held a short distance apart under a helium atmosphere. Carbon evaporated from the anode re-condensed at cathode and form carbon nanotubes.

Sol-gel synthesis

The sol-gel process is a versatile solution process for making ceramic and glass materials. In general, the sol-gel process involves the transition of a system from a liquid "sol" into a solid "gel" phase. A sol is a dispersion of the solid particles (~ 0.1-1 mm) in a liquid. The starting materials used in the preparation of the "sol" are usually inorganic metal salts or metal organic compounds such as metal alkoxides. In a typical sol-gel process, the precursor is subjected to a series of hydrolysis and polymerisation reactions to form a colloidal suspension, or a "sol".

Ion Sputtering

In this method, accelerated ions such as Ar^+ are directed toward the surface of a target to eject atoms and small clusters from its surface. The ions are carried to the substrate under a relatively high pressure (~1mTorr) of an inert gas, causing aggregation of the species. Nanoparticles of metals and alloys as well as semiconductors have been prepared using this method.

Solvothermal Synthesis

The solvothermal method provides a means of using solvents at temperatures above their boiling points, by carrying out the reaction in a sealed vessel. The pressure generated in the vessel due to the solvent vapors elevates the boiling point of the solvent. Typically, solvothermal methods make use of solvents such as ethanol, toluene, and water, and are widely used to synthesize zeolites, inorganic open-framework structures, and other solid materials.

Sonochemical Synthesis

In order to carry out sonochemical reactions, a mix of reagents dissolved in a solvent is subjected to ultrasound radiation (20 kHz–10 MHz). Acoustic cavitation leads to the creation, growth, and collapse of bubbles in the liquid medium. The creation of bubbles is due to the suspended particulate matter and impurities in the solvent. The growth of a bubble by expansion leads to the creation of a vacuum that induces the diffusion of volatile reagents into the bubble. The growth step is followed by the collapse of the bubble which takes places rapidly accompanied by a temperature change of 5,000–25,000K in about a nanosecond.

Micelles and Microemulsions

Reverse or inverted micelles formed by the dispersion of water in oil, stabilized by surfactants are useful templates to synthesize nanoscale particles of metals, semiconductors, and oxides [410–413]. This method relies on the ability of surfactants in the shape of truncated cones (like cork stopper), to trap spherical droplets of water in the oil medium, and thereby forming micelles. A micelle is designated inverse or reverses when the hydrophilic end of the surfactant points inward rather than outward as in a normal micelle.

Although these strategies are widespread demonstrated effective methods to fabricate $PbWO_4$ nanostructures with various morphologies, large scale application of these methods has been limited due to some shortcomings, such as some methods need expensive templates or surfactants, and others needing complicated process, or even tedious procedures.

Recently, significant efforts have been devoted to develop green method that take into account human and environmental impact in the selection of reactants and the reaction conditions for material fabrication. Many recent studies have demonstrated that hydrothermal process is an effective and versatile route for the synthesis of nanostructures having low-cost, high efficiency and good potential for high-quantity production [31]. A brief description of hydrothermal method is given in Chapter 2.

It is believable that controlling the morphology and architecture of $PbWO_4$ crystals is expected to be effective in modifying their related properties for practical application. The shape, phase, and size of inorganic nanocrystals are important elements in varying their electrical, optical, and other properties, so control over these elements have become a hot research topic in recent years. The controlled synthesis of inorganic nano- and microcrystals with specific size, shape and structure is of fundamental significance in modern material science and engineering because the size, shape and structure could determine not only the relevant optical, electronic and magnetic properties of the materials but also the performances of those material-based devices for applications. Recently, many efforts have been made to synthesize tungstate crystals with controlled morphologies because of their excellent luminescent properties and promising applications.

1.4 Crystal Structure of $PbWO_4$

At room temperature, $PbWO_4$ has two different possible polymorphs, tetragonal stolzite or scheelite structure with space group $I4_1/a$ and monoclinic wolframite or raspite structure with space group $P2_1/c$ [32]. Two different crystal structures of $PbWO_4$ are shown in below image.

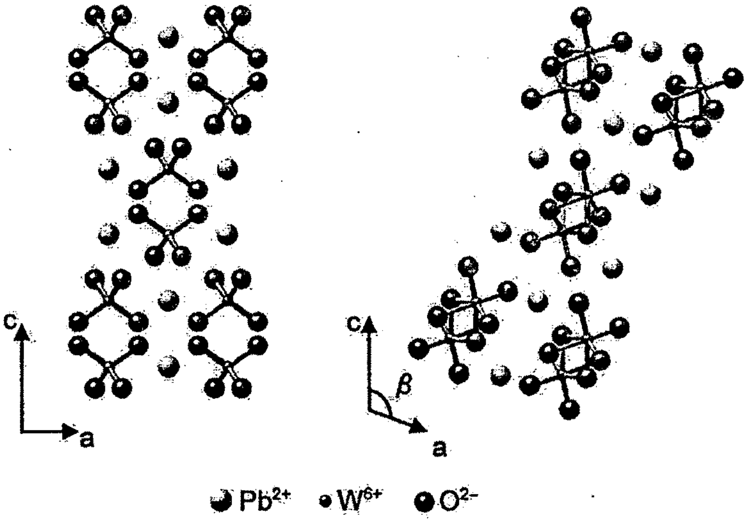

(a) scheelite (b) raspite

[Ref. M. Itoh and M. Fujita, Physical Review B, Vol. 62, Number 19]

1.4.1 Scheelite

In the scheelite structure, W ions are in tetrahedral O-ion cages and isolated from each other. Each Pb^{2+} cation is surrounded by eight oxygen ions. The connection between cation Pb^{2+} and anion WO_4^{-2} is ionic and the connection between W^{6+} and O^{2-} in the oxianion complex is covalent.

1.4.2 Raspite

In the raspite structure, the coordination number of W is six and WO_6^{-6} octahedra form a chain by edge sharing. Each Pb^{2+} cation is coordinated to seven oxygen ions. The monoclinic form of $PbWO_4$ (raspite-type) can be treated as a distortion of the tetragonal form of $PbWO_4$ (scheelite-type). It is known that the raspite phase is a metastable and minority form under normal conditions [33]. The raspite $PbWO_4$ has not yet been successfully prepared in the laboratory and is obtained as a natural crystal except by C.Zheng [34].

From the structure point of view, in spite of the very small volume difference of 0.53% between the raspite and scheelite forms, the difference in the cation coordination is remarkable. As displayed in Fig.1, which gives the atomic structures of both raspite and scheelite, the W atoms in the scheelite structure are at the tetrahedral O-atom cages and isolated from one another, whereas in the raspite phase, two W atoms share two O ions to form a chain of edge-shared octahedra. Each Pb ion is surrounded by seven O ions in the raspite structure, whereas in the scheelite structure, the number of the surrounding O ions to each Pb ion is eight [35]. It was reported that displacement of O ions in such a phase transformation is considered small, while that of the cations is relatively large. The body-center primitive tetragonal ($Z = 4$) of $PbWO_4$ the total number of degrees of freedom for the atomic vibrations is $3N = 72$. In $PbWO_4$, the Pb^{2+} ions and the tetrahedral $[WO_4]^{2-}$ ions are at the S_4-symmetry crystallographic positions [36].

1.5 Doping with Trivalent Rare Earth Ions (RE^{3+})

In order to use $PbWO_4$ crystal as scintillation detector its radiation hardness should have high value.The radiation damage in $PbWO_4$ crystals is caused by host structural defects called color centers e.g. Oxygen vacancies (V_o) and Lead vacancies (V_{Pb}) [37]. Such vacancies are produced due to high synthesis temperature during crystal growth which introduces local charge imbalance. So to improve radiation hardness by decreasing concentration of these vacancies, low temperature hydrothermal method is preferable. To balance charge these vacancies act as charge traps centers. V_o and V_{Pb} act as electron and hole traps respectively. Out of these two, V_o is mainly responsible for radiation damage in $PbWO_4$. So in order to decrease V_o, post-growth annealing at high temperature is required.

Doping with trivalent rare earth ion is another approach which minimizes the charge imbalance produced by vacancies. In 1997, Kobayashi et al. first reported that La^{3+} doping into $PbWO_4$ could improve both the radiation hardness and the transmittance in the short-wavelength region [38]. Since then, doping with different impurity ions, especially rare-earth ions (RE^{3+}), has become the focus of studies to ameliorate its scintillating characteristics.

1.5.1 Cerium

Cerium is the most abundant member of the series of elements known as lanthanides or rare earths. Cerium is characterized chemically by having two stable valence states one is Ce^{4+}, *ceric,* and the other is Ce^{3+},*cerous.* The ceric ion is a powerful oxidizing agent but when associated with the strongly coordinating ligand, oxygen, is completely stabilized and induced cerium oxide, $Ce^{4+}O_2$, (also called ceria) is the form of cerium most widely used. The ground state of all the Lanthanide atoms is probably either [Xe] $4f^n5d^1$ or [Xe] $4f^{\,n+1}$ where the increase in n from 0 to 14 corresponds to the change from La (Z=57) through to Lu (Z=71).

Cerium is the second and most reactive member of the lanthanides series. It is electro-positive in nature and become predominantly chemically reactive due to the low ionization potential for the removal of the three most weakly bound electrons. For all lanthanides the most stable state is a trivalent one, Ln^{3+}, with [Xe]$4f^n$; i.e. for Ce^{3+}, [Xe]$4f^1$. Rare earth ions have unfilled optically active 4f electrons screened by outer electronic filled shells. Because of these unfilled shells, this kind of ion is usually called *paramagnetic ions.*

The rare earth (RE) ions most commonly used for applications as phosphors, lasers, and amplifiers. The cerium atom (Z=58), which has an outer electronic configuration $5s^2$ $5p^6$ $5d^1$ $4f^1$ $6s^2$. These atoms are usually incorporated in crystals as divalent or trivalent cations. In trivalent ions 5d, 6s, and some 4f electrons are removed and so $(RE)^{3+}$ ions deal with transitions between electronic energy sublevels of the $4f^n$ electronic configuration. Divalent lanthanide ions contain one more f electron (for instance, the Eu^{2+} ion has the same electronic configuration as the Gd^{3+} ion, the next element in the periodic table but, at variance with trivalent ions, they to show f→d inter-configurational optical transitions. This aspect leads to quite different spectroscopic properties between divalent and trivalent ions. The $4f^n$ electrons are, in fact, the valence electrons that are responsible for the optical transitions.

The number of 4f electrons (n) in trivalent lanthanide ions

Ion	n
Ce^{3+}	1
Pr^{3+}	2
Nd^{3+}	3
Pm^{3+}	4
Sm^{3+}	5
Eu^{3+}	6
Gd^{3+}	7
Tb^{3+}	8
Dy^{3+}	9
Ho^{3+}	10
Er^{3+}	11
Tm^{3+}	12
Yb^{3+}	13

These valence electrons are shielded by the 5s and 5p outer electrons of the $5s^2$ $5p^6$ less energetic configurations. Because of this shielding effect, the valence electrons of Ce^{3+} ion are weakly affected by the ligand ions in $PbWO_4$ crystals; a situation results the case of a weak crystalline field. For Weak crystalline field: $H_{CF} \leq H_{SO}$, H_{ce}, H_O. Consequently, the spin–orbit interaction term of the free Ce^{3+} ion Hamiltonian is dominant over the crystalline field Hamiltonian term. In this case, the energy levels of the free Ce^{3+} ion are only slightly perturbed (shifted and split) by the crystalline field. This causes the $^{2S+1}L_J$ states of the $(RE)^{3+}$ ions to be slightly perturbed when these ions are incorporated in crystals. The effect of the crystal field is to produce a slight shift in the energy of these states and to cause additional level splitting. However, the amount of this shift and the splitting energy are much smaller than the spin–orbit splitting, and thus, the optical spectra of $(RE)^{3+}$ ions are fairly similar to those expected for free ions. The free ion wavefunctions are then used as basis functions to apply perturbation theory, H_{CF} being the perturbation Hamiltonian over the $^{2S+1}L_J$ states (where S and L are the spin and orbital angular momenta and $J = L + S$). This approach is generally applied to describe the energy levels of trivalent rare earth ions, since for these ions the 4f valence electrons are screened by the outer $5s^2\ 5p^6$ electrons. These electrons partially shield the crystalline field created by the B ions.

References

1. G. Blasse and B.C. Grabmaier "Luminescent Materials", springer-verlag, 226p, 1994.
2. R. Deych, J. Dobbs, S. Marcovic and B. Tuval , Proc. of the int. conf. on Inorganic Scintillator and Their application,SCINT-95, Netherlands, Delft, 36, 1996.
3. R. Shaw and G.F. Claringull, Am. Mineral, 40, 933, 1955.
4. F.A. Kroger, Some Aspects of the Luminescence of Solids, Elsevier, Amsterdam, New York, 1948.
5. P. Lecoq, I. Dafinei , E. Auffray , M. Schneegans ,V. Korzhik , O.V. Missevitch, V.B. Pavlenko, A.A. Fedorov, A.N. Annenkov, V.L. Kostylev, Nucl. Instrum. Meth. A 365, 291, 1995.
6. M. Kobayashi, M. Ishii, Y. Usuki, Nucl. Instrum. Methods Phys. Res. A 406 442,1998.
7. K. Hara, M. Ishii, M. Kobayashi, M. Nikl, H. Takano, M. Tanaka, K. Tanji, Y. Usuki, Nucl. Instrum. Methods Phys. Res. A, 414, 325, 1998.
8. Kobayashi, M., Ishii, M.; Usuki, Y. Nucl. Instrum. Methods Phys.Res., Sect. A, 406, 442,1998.
9. Hara, K., Ishii, M., Kobayashi, M., Nikl, M., Takano, H., Tanaka, M., Tanji, K., Usuki, Y. Nucl. Instrum. Methods Phys. Res., Sect. A 414 (1998) 325.
10. G. Blasse, L.H. Brixner, Chem. Phys. Lett. 409 (1990) 173.
11. Y. Huang, Q. Feng, Y. Yang, H.J. Seo, Phys. Lett. A 336 (2005) 490– 497.
12. Z. Qi, C. Shi, D. Zhou, H. Tang, T. Liu, T. Hu, Phys. Rev. B: Condens. Matter 307 (2001) 45–50.
13. S. Oishi, M. Hirao, Bull. Chem. Soc. Jpn. 63 (1990) 984.

14. W. Cho, M. Yashima, M. Kakihana, A. Kuso, T. Sakata, M. Yoshimura, Appl. Phys. Lett. 66 (1995) 1022.
15. K. Nitsch, M. Nikl, S. Ganschow, P. Reiche, R. Uecker, J. Cryst. Growth 165 (1996) 163.
16. N. Senguttuvan, P. Mohan, S.M. Babu, C. Subramanian, J. Cryst. Growth 183 (1998) 391– 397.
17. A.V. Denisov, V.T. Gabrielyan, J.O. Punin, O.S. Grunsky, N.A. Sennova, J. Cryst. Growth 275 (2005) 697–701.
18. K. Tanji, M. Ishii, Y. Usuki, K. Hara, H. Takano, A. Senguttuvan, J. Cryst. Growth 204 (1999) 505.
19. D. Schultze, K.Th. Wilke, Ch. Waligorn, Z. Anorg, Allg. Chem. 352 (1967) 184.
20. S. Nobuhiro, K. Akihiko, K. Tadayoshi, Bull. Chem. Soc. Jpn. 69 (1996) 1241–1245.
21. K. Nitsch, M. Nikl, M. Rodov'a, S. Santucci, Phys. Status Solidi A 179 (2000) 261–264.
22. J. Geng, J.-J. Zhu, D.-J. Lu, H.-Y. Chen, Inorg. Chem. 45 (2006) 8403–8407.
23. D. Chen, G. Shen, K. Tang, Z. Liang, H. Zheng, J. Phys. Chem. B 108 (2004) 11280–11284.
24. Guizhen Wang, Chuncheng Hao Materials Research Bulletin 44 (2009) 418–421.
25. Jeong Ho Ryu, Jong-Won Yoon, Kwang Bo Shim, Solid State Communications 133 (2005) 657–661.
26. HuaTang, Changsheng Li, Haojie Song, Xiaofei Yang and Xuehua Yan, CrystEngComm,13(2011) 5119–5124.
27. C. An, K. Tang, G. Shen, C.Wang,Y. Qian, Mater. Lett. 57 (2002) 565–568.

28. Guangyu Chen, Liangbao Yang, and Jinhuai Liu, Cryst. Res. Technol. 44, No. 7, (2009) 736 – 740.
29. Wei Zhao, Xinyu Song, Guozhu Chen, Guangru Tian, Sixiu Sun Materials Letters 63 (2009) 285–288.
30. D.Tawde, M.Srinivas & K.V.R.Murthy, Physica Status Solidi A, Vol.208, Issue 4, 803- 807, 2011.
31. W.X. Zhang, X.G. Wen, S.H. Yang, Y. Berta, Z.L. Wang, Adv. Mater. 15 (2003) 822.
32. T. Fujita, I. Kawada, and K. Kato, Acta Crystallogr. Sect. B: Struct. Sci. 33(1977)162.
33. R. Shaw and G. F. Claringbull, Am. Mineral. 40 (1955) 933.
34. Chunhua Zheng, Chenguo Hu, Xueyan Chen, Hong liu, Yufeng Xiong, Jing Xu, Buyong Wana and Linyong Huang, CrystEngComm,12 (2010) 3277–3282.
35. L. S. Cavalcante, J. C. Sczancoski, V. C. Albarici, J. M. E. Matos, J. A. Varela, and E. Longo, Mater. Sci. Eng., B 150 (2008) 18.
36. A.A. Kaminskii, C.L. McCray, H.R. Lee, S.W. Lee, D.A. Temple, T.H. Chyba, W.D. Marsh, J.C. Barnes, A.N. Annanenkov, V.D. Legun, H.J. Eichler, G.M.A. Gad, K. Ueda, Opt. Commun. 183 (2000) 277.
37. R.Y. Zhu, et al., Nucl. Instr. and Meth. A 376 (1996) 319.
38. M. Kobayashi, Y. Usuki, M. Ishii, T. Yazawa, K. Hara: Nucl. Instrum. Methods Phys. Res. A 399 (1997) 261.